BBA - Molecular Basis of Disease 1865 (2019) 1201–1213

Contents lists available at ScienceDirect

BBA - Molecular Basis of Disease

journal homepage: www.elsevier.com/locate/bbadis

Epstein–Barr virus noncoding RNAs from the extracellular vesicles of nasopharyngeal carcinoma (NPC) cells promote angiogenesis via TLR3/RIG-I-mediated VCAM-1 expression

Shiyue Cheng[a,b], Zhi Li[a,b,*], Junju He[a,b], Shujun Fu[a,b], Yumei Duan[c], Qin Zhou[d], Yuanliang Yan[e], Xiaoyu Liu[f], Liyu Liu[a,b], Chang Feng[a,b], Lu Zhang[a,b], Jiang He[a,b], Yuezhen Deng[a,b], Lun-Quan Sun[a,b,*]

[a] Center for Molecular Medicine, Xiangya Hospital and Collaboration Innovation Center for Cancer Medicine, Central South University, China
[b] Key Laboratory of Molecular Radiation Oncology of Hunan Province, China
[c] Department of Pathology, Xiangya Hospital, Central South University, China
[d] Department of Oncology, Xiangya Hospital, Central South University, China
[e] Department of Pharmacy, Xiangya Hospital, Central South University, Changsha 410008, China
[f] Shanghai Institute of Medical Image, Fudan University, Shanghai 200032, China

ARTICLE INFO

Keywords:
Angiogenesis
Epstein–Barr virus
Nasopharyngeal carcinoma
Noncoding RNA
VCAM-1

ABSTRACT

Viral noncoding RNAs (Epstein–Barr virus-encoded RNAs, EBERs) are believed to play a critical role in the progression of lymphoma and nasopharyngeal carcinoma (NPC). However, the accurate mechanisms accounting for their oncogenic function have not been elucidated, especially in terms of interaction between tumor cells and mesenchymal cells. Here, we report that, in addition to NPC cells, EBERs are also found in endothelial cells in Epstein–Barr virus (EBV)-infected NPC parenchymal tissues, which implicates NPC-derived extracellular vesicles (EVs) in transmitting EBERs to endothelial cells. In support of this hypothesis, we first ascertained if EBERs could be transferred to endothelial cells via EVs isolated from NPC culture supernatant. Then, we clarified that EVs-derived EBERs could promote angiogenesis through stimulation of VCAM-1 expression. Finally, we explored the involvement of EBER recognition by TLR3 and RIG-I in NPC angiogenesis. Our observations collectively illustrate the significance and mechanism of EVs-derived EBERs in angiogenesis and underlie the interaction mechanisms between EBV-infected NPC cells and the tumor microenvironment.

1. Introduction

Viral noncoding RNAs (Epstein–Barr virus-encoded RNAs, EBERs) are the most abundant EBV transcripts (about 10^7 copies per cell) during latent EBV infection in a variety of cell types. Owing to their expression abundance and universal existence in all the 3 forms of latent infection, EBERs have been intensively investigated since their discovery by Lernar [1,51].

EBERs comprise EBER1 and EBER2 (167 and 172 nt long, respectively) [2] and are reported to be associated with proteins recognizing their double-stranded secondary structure, such as TLR3 and RIG-I [3,4]. Furthermore, the interacting proteins of both of EBERs include La [1] and PKR [5,6], which aids in proper folding of RNA Poll III transcripts and confers resistance to apoptosis, respectively. Moreover, relocalization of L22 from the nucleolus to the nucleoplasm via interaction with EBER1 was observed [7,8], which might result in a depletion of the protein from ribosomes. In addition, AUF1 sequestration attributable to interaction with EBER1 may leads to interference with the stability of AU-rich element-containing mRNAs or suppressing senescence [9,10]. In terms of EBER2, interaction with PAX5 was recently reported to be involved in the lytic replication in the EBV infected Burkitt lymphoma cells [11].

With regard to the oncogenic roles in solid tumors of epithelial origin, studies have indicated that EBERs are suggested to promote neoplasia via IGF [12]. We recently found that EBERs could promote NPC progression via TLR3 and RIG-I-mediated cancer-related inflammation [13,14]. However, contradictory observations regarding the capability of EBERs in the transformation of lymphoma and NPC

* Corresponding authors at: Center for Molecular Medicine, Xiangya Hospital and Collaboration Innovation Center for Cancer Medicine, Central South University, China.
E-mail addresses: peries@csu.edu.cn (Z. Li), lunquansun@csu.edu.cn (L.-Q. Sun).

https://doi.org/10.1016/j.bbadis.2019.01.015
Received 9 September 2018; Received in revised form 30 December 2018; Accepted 13 January 2019
Available online 16 January 2019
0925-4439/

exist [8,15,16]. Furthermore, EBERs are reported to be present in fractions related to exosomes released by EBV-transformed cells [17], which might account for the pathogenesis of active EBV infections characterized by cytokinemia [3].

Tumor-associated neovasculature, generated by the process of angiogenesis, contributes to the rapid growth of tumor by tilting the balance toward activating angiogenic factors such as vascular endothelial growth factor (VEGF) and fibroblast growth factor (FGF) and inhibiting angiogenesis inhibitors such as TSP-1 and angiostatin [18,19]. In addition to supplying surrounding tissues with oxygen and nutrients, angiogenesis activates endothelial cells in response to inflammatory stimulus to increase the expression of adhesion molecules, including ICAM, VCAM-1, E-selectin, CD105, and CD54, and this process facilitates the interaction between neutrophils and endothelial cells [20]. Of note, some of these adhesion molecules are not just involved in the process of cell recognition and adhesion, they can also promote angiogenesis *in vitro* and *in vivo*, as has been demonstrated with soluble VCAM-1 and E-selectin [21]. However, the mechanism underlying this process remains not fully understood.

Cells can communicate with neighboring or distant cells through the secretion of extracellular vesicles (EVs). Those vesicles are composed of exosomes and ectosomes (30–150 nm and 100–1000 nm in diameter, respectively), with a lipid bilayer containing transmembrane proteins, which encloses the cytosolic proteins and RNA. EVs have been shown to participate in many facets of cancer progression and treatment, including metastasis, therapy-induced resistance, and angiogenesis [22]. Importantly, in addition to proteins and mRNAs, miRNAs and other noncoding RNAs are also in active EV cargoes. Several groups have recently observed tumor cell-released EV-mediated secretion of specific miRNAs or lncRNAs in the tumor microenvironment to be responsible for cancer-promoting angiogenesis [23–27]. However, limited information is available on the impact of viral noncoding RNAs on promoting cancer angiogenesis in the form of tumor cell-released EVs.

To elucidate the accurate mechanisms accounting for the oncogenic function of EBERs, especially in terms of interaction between tumor cells and mesenchymal cells, the present investigation attempts to establish if EBV-positive NPC cells could transmit EBERs to surrounding endothelial cells via the secretion of EVs, leading to building a tumor-promoting microenvironment via augmented angiogenesis.

2. Materials and methods

2.1. Cell lines and cell culture

C666-1 is an NPC cell line consistently harboring Epstein-Barr virus [28]. CNE1, HNE2 and CNE2, are EBV negative NPC cell lines. CNE1-EBERs, HNE2-EBERs are stable EBERs-integrated NPC cell lines and CNE2-LMP1 is a stable EBERs-integrated NPC cell line constructed in our lab. All NPC cell lines are maintained in RPMI 1640 (Invitrogen, Carlsbad, CA, USA) supplemented with 10% fetal bovine serum (FBS), 100 units/mL penicillin, and 100 mg/mL streptomycin. The Ethical Review Committee approved the study and the parturient provided written informed consent with regard to experiments using primary Human umbilical vein endothelial cells (HUVECs). HUVECs were isolated from human umbilical cord, which was provided by maternity department of Xiangya Hospital, Changsha, China. HUVECs were maintained in RPMI 1640 (Invitrogen) supplemented with 10% FBS, 10 ng/mL EGF, and 10 ng/mL FGF (Peprotech, Rocky Hill, NJ, USA). Isolated HUVECs were identified by their typical cobblestone morphology and by immunostaining for von Willebrand factor. All cell lines were maintained at 37 °C with 5% CO_2.

2.2. Reagents and transfection

EBERs expression plasmid used in this paper has been described previously [13]. TLR3 and RIG-I shRNA plasmids used in this paper have been described previously [13,14]. Cells were transfected with plasmids using ViaFect reagent (Promega, Madison, WI, USA) following the manufacturer's instructions. Briefly, 3×10^5 cells seeded in a six-well plate were transfected with 2 μg plasmids the following day. Control siRNA and siRNA targeting VCAM-1 were designed and provided by RiBo Biotech (Guangzhou, China). Control ASO was manufactured and modificated by RiBo Biotech based on Nara Lee's descriptions [11]. U0126, a MEK1/2 inhibitor, was purchased from Sigma (St. Louis, USA). ASO targeting EBER1 were designed, synthesized and modificated by RiBo Biotech. The targeting sequences of siRNA/shRNA and ASOs were listed in Supplementary Table S1. Cells were transfected with siRNA or ASOs following the manufacturer's instructions. Briefly, cells were transfected once with 50 nM siRNA or 200 nM ASOs for efficient knockdown of target genes.

2.3. EVs isolation and characterization

2.3.1. Ultracentrifugation

FBS was purified by ultracentrifugation at 100,000 ×*g* for 3 h at 4 °C. Then the precipitate at the bottom (EVs fraction) was discarded and the remaining supernatant were used as EVs free FBS for following experiments.

2.3.2. ExoQuick precipitation

Exosomes produced from C666-1 cells were isolated from conditioned culture medium supplemented with 10% FBS by ultracentrifugation using by the ExoQuick exosome precipitation solution according to the manufacturer's recommendations (System Biosciences, Mountain View, CA, USA). Briefly, 1/5 volume of ExoQuick Solution was added to conditioned culture medium and refrigerated at 4 °C overnight. The mixture was centrifuged at 1500 ×*g* for 30 min, and the supernatant was removed by aspiration. The pelleted fraction was resuspended in nuclease-free water. Once the exosomes were obtained, we detected the expression of TSG101 (an exosome marker protein) by western blot assay and examined the exosomes by scanning electron microscopy analysis. Isolated EVs were used immediately, or were resuspended in 50–100 μL of PBS and stored at −80 °C.

2.4. Transmission electron microscopy on EVs

10 μL of EVs suspension in 1× PBS was dried onto freshly glow discharged 200 mesh formvar-carbon-coated copper grids, negatively stained with 2% aqueous uranyl acetate and observed with a Tecnai G2 Spirit TWIN transmission electron microscope (TEM) (FEI, Hillsboro, Oregon, USA).

2.5. Size distribution analysis of C666-1 derived EVs

EVs derived from C666-1 culture supernatant were diluted in 1 mL PBS, and size distribution was analyzed with the Zetasizer Nano ZEN3690 (Malvern Instruments Ltd., Malvern, UK) at 37 °C according to the manufacturer's instructions.

2.6. Fluorescence labeling of EVs

EVs from C666-1 were labeled using PKH67 green fluorescent cell linker kit (Sigma-Aldrich, St. Louis, MO, USA) according to the manufacturer's recommendations. Briefly, EVs were dissolved in 1 mL Diluent C, and 4 μL PKH67 was added in 1 mL Diluent C separately. Then buffers were mixed and left to stand at room temperature for 5 min, after which the reaction was stopped with FBS without EVs. The samples were then transferred to a 100 kDa Amicon Ultra centrifugal filter (Merck Millipore, Billerica, MA, USA) and centrifuged at 3000 ×*g* for 15 min. Finally, the sample was washed 3 times with 5 mL PBS and resuspended in PBS until use. Prepared EVs were then co-cultured with HUVECs for 24 h, then the co-cultured cells were photographed using

confocal microscope (Leica, SP5 X, Wetzlar, Germany).

2.7. Transwell migration assay

The assay used 24-well Transwell plates with 8-μm-pore polycarbonate filters (Corning Costar, Corning, NY, USA). Transwell inserts were coated with 100 μL diluted (1:10 with RPMI) Matrigel (BD Biosciences, San Diego, CA, USA) and solidified at 37 °C for 1 h. Cells (3×10^4) resuspended with 200 μL serum-free medium were seeded onto the upper chamber, and 700 μL complete medium with FBS was added to the lower chamber. The inserts were removed after incubation for 48 h at 37 °C and 5% CO_2. The cells were then stained with crystal violet and counted by viewing under a microscope of 5 random microscopic fields.

2.8. Co-culture

Six-well Transwell plates with 0.4-μm pore membrane inserts (Corning Costar, Corning, NY, USA) were used. C666–1 cells were seeded unto the upper chamber, and the lower chamber was seeded with HUVECs and these cells were co-cultured for 1 week.

2.9. In vitro HUVEC tube formation assay

Matrigel (50 μL/well) was applied in 96-well plates and incubated for 1 h at 37 °C. The cell suspension (50 μL) was seeded onto Matrigel. After incubation for 8 h, photomicrographs of each well were taken under light microscopy, and the total tube area was quantified as mean pixel density obtained from image analysis of 5 random microscopic fields using ImageJ software (http://rsb.info.nih.gov/nih-image/).

2.10. Matrigel plug assay

All animal experiments were conducted at the Central South University in compliance with Chinese legislation for animal care. The 6-week-old female nude mice were used in the assay (Slac Laboratory Animal, Shanghai, China). HUVECs (2×10^6; transfected EBERs or pcDNA-3.1) suspended in 300 μL complete medium were injected subcutaneously with 300 μL growth factor reduced Matrigel (BD Biosciences). After 1 week, the Matrigel plugs were harvested and processed for analysis. All studies were performed following guidelines approved by the Experimental Animal Ethics Committee of Central South University.

2.11. Immunohistochemistry (IHC) of matrigel plugs

Plugs were fixed with formalin, cut into 4-μm sections and then mounted on slides, deparaffinized in xylene, and rehydrated through a graded alcohol series to water. For antigen retrieval, slides were heated in 0.01 mol/L citrate buffer (pH 6.0). After the slides were cooled to room temperature, endogenous peroxidase was blocked with 30% H_2O_2. The slides were washed with PBS and treated with 5% BSA to block nonspecific binding sites. This was followed by incubation with an anti-CD31 antibody (Ab9498, Abcam, Cambridge, MA, USA) at 4 °C overnight. After PBS rinses, the slides were incubated with the HRP-conjugated secondary antibody (Abcam) for 30 min at room temperature. Immunostaining was performed using DAB (Abcam). Finally, nuclei were counterstained with hematoxylin for 1 min and examined under a microscope. The quantification of IHC staining density was performed by ImageJ software and calculated on the basis of the average staining intensity and the percentage of positively stained cells.

2.12. Scratch wound healing assay

Confluent cell monolayers were scratched with a sterile pipette tip. Then, the cells were washed with D-Hanks solution to remove any floating cells. At time 0 and after 24 or 48 h, the migrated distance were examined and photographed using a phase-contrast microscope (Leica DMI3000B, Wetzlar, Germany).

2.13. Qiagen RT^2 profiler PCR array and qRT-PCR

Total RNA was prepared with Trizol (Invitrogen, Carlsbad, CA, USA) from HUVECs transfected with control or EBERs expression plasmid for 24 h. RNA samples were reverse transcribed using the PrimeScript RT reagent kit with gDNA Eraser (Takara & Clontech, Tokyo, Japan). Quantitative real-time PCR (qRT-PCR) analysis was performed using the CFX-96 real-time PCR system (Bio-Rad, Hercules, CA, USA). For PCR array experiments, an RT^2 Profiler PCR array was used to simultaneously examine the mRNA levels of genes closely associated with angiogenesis, including 5 housekeeping genes, in 96-well plates following the manufacturer's protocol (PAHS-024Z, PAHS-072Z). Heatmap of differential expression of genes were generated using the web interface (http://hemi.biocuckoo.org). Volcano plots of differential expression of genes were obtained and analyzed on the Qiagen website (http://pcrdataanalysis.sabiosciences.com/pcr/arrayanalysis.php). The primers were listed in Table S2.

2.14. Western blot analysis

Protein of NPC cell lines and HUVECs were prepared in a standard RIPA buffer containing proteinase and phosphatase inhibitors (Roche, Indianapolis, IN, USA). Then prepared protein were separated via SDS-PAGE and transferred to NC membranes (Pierce Biotechnologies Inc., Rockford, IL, USA). The primary antibodies anti-E-selectin (ab18981, Abcam), VCAM-1 (ab134047, Abcam), p42 MAP Kinase (Erk2) (9108S, CST, CA, USA), p44/42 MAPK (Erk1/2) (4695S, CST, CA, USA) and phosphorylated ERK (9101S, CST, CA, USA) were used for the assay, and the bound antibodies were detected with HRP-conjugated secondary antibodies (Abcam). Densitometric analysis of WB results were performed with ImageJ software.

2.15. In situ hybridization

In situ hybridization (ISH) was performed using the EBER HRP-conjugated probe and DAB as the substrate from the ISH kit (Life Technologies, Carlsbad, CA, USA), according to the manufacturer's instructions.

2.16. Luciferase assay

Reporter assay was conducted according to the manufacturer's directions (Promega, Fitchburg, WI, USA). The luciferase reporter plasmids were co-transfected with pRL-SV40 to correct for variations in transfection efficiency. The relative luciferase activity was normalized to the value of pRL-SV40 activity. The VCAM-1 promoter sequence (Transcriptional start site [TSS] ± 1 kb) was cloned into luciferase reporter plasmid in front of luciferase CDS sequence.

2.17. Statistical analyses

Statistical analyses were performed using SPSS 18.0 (SPSS) and GraphPad Prism, version 5. Results are expressed as means ± SD. For comparisons between groups, statistical analyses were performed using the Mann–Whitney test. Differences with P values of <0.05 were considered significant.

3. Results

3.1. EBERs are present in epithelial cells within NPC parenchymal tissues

Given that EBV-infected NPC cells can communicate with

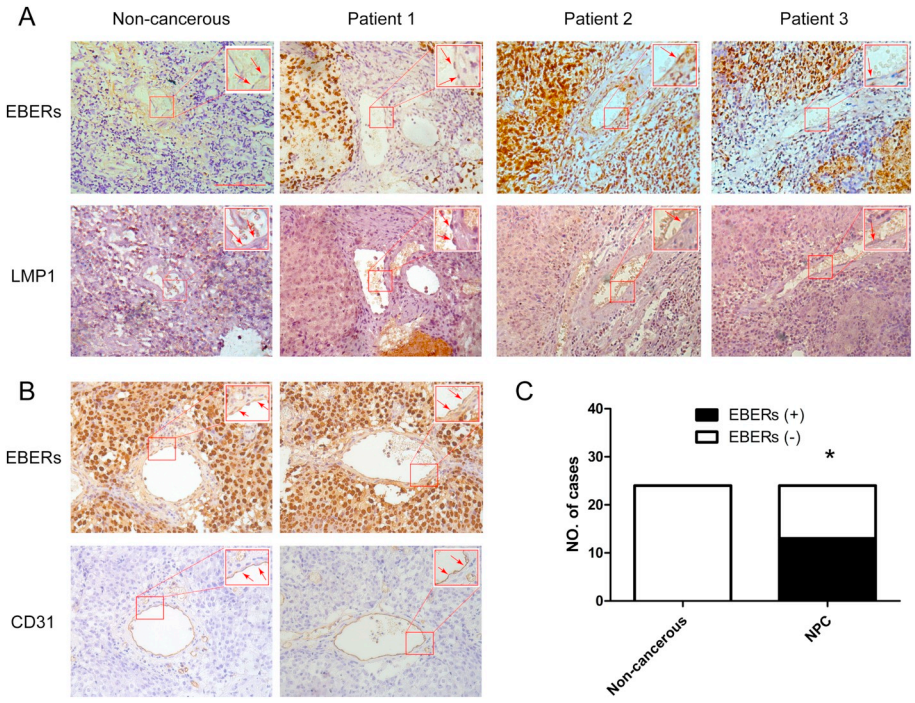

Fig. 1. EBERs are present in endothelial cells within NPC parenchymal tissues. (A) Serial sections of 24 non-cancerous and 24 NPC tissues with discernible capillaries were subjected to IHS staining for EBERs or IHC staining for LMP1. Representative sections of staining of EBERs (upper panel) and LMP1 (lower panel) is depicted (patient 1 represents EBERs negative case, patient 2 and 3 represent EBERs positive case). The enlarged picture presents the cross-section of a complete capillary, and the arrows point to endothelial cells with or without EBERs or LMP1. The scale bar indicates 100 μm. (B) Analysis of endothelial marker CD31 expression by Immunohistochemical (IHC) on consecutive sections on which EBER ISH was performed. The enlarged picture presents the cross-section of a complete capillary, and the arrows point to endothelial cells co-stained with EBERs and CD31. Here exemplified are two representative patients' staining results (patient 4 and 5). The scale bar indicates 100 μm. (C) Histogram presents number of cases with EBERs-positive or EBERs-negative endothelial cells of non-cancerous and NPC tumor parenchymal tissues (n = 24 respectively). (C) *P < 0.05, Mann–Whitney test.

endothelial cells [23], we tried to explore the possible role of EBERs in the regulation of endothelial cells. ISH staining of NPC cells indicated that EBERs were frequently present in endothelial cells in the vicinity of EBV-positive NPC cells (upper panel of Fig. 1A, patient 2 and patient 3), whereas EBERs could not be detected in endothelial cells of tumor parenchymal tissue that was not infected by EBV (upper panel of Fig. 1A, non-cancerous, Supplementary Fig. 1). Recent observations indicate the latent membrane protein 1 (LMP1), a primary oncoprotein encoded by EBV that plays a key role in both the initiation and progression of NPC [52,53], could be transmitted via exosomes and induce expression of the EGFR [23]. Interestingly, analysis of EBV LMP1 expression by Immunohistochemical (IHC) on consecutive sections on which EBER ISH was performed indicated the absence of LMP1 in EBER-positive endothelial cells (lower panel of Fig. 1A, Supplementary Fig. 1). *In situ* hybridization (ISH) of EBERs and immunohistochemistry (IHC) of LMP1 with EBERs or LMP1 stable expression NPC cell line validated our experimental system (Supplementary Fig. 1). These observations suggest that EBERs are probably transferred from EBV-positive NPC cells to surrounding endothelial cells. We further confirmed this conclusion via confirmation of co-staining of CD31 and EBERs in the same endothelial cell (Fig. 1B). Furthermore, a deeper investigation indicated in 13 of 24 NPC tissue samples (compared to 0 of 24 in non-cancerous group), EBERs were present in endothelial cells of tumor parenchymal tissues (Fig. 1C, patient 2 and 3 of Fig. 1A), whereas EBERs staining was negative in endothelial cells of the rest NPC tissue samples (Fig. 1C, patient 1 of Fig. 1A).

3.2. EBERs are transferred to surrounding endothelial cells via EVs released by EBV-positive NPC cells

On the basis of our observation that EBERs could localize in endothelial cells, as well as the previous literature describing the release of EBERs into culture supernatant from EVs [17,24–27,29,30], we reasoned that EBERs present in endothelial cells might originate from EVs released from NPC cells. To test this hypothesis, we first set up transwells in which cells of the EBV-positive NPC line C666-1 were separated by a porous 0.4-μm membrane from HUVECs. EVs and other soluble factors, but not cells, could migrate across these membranes. Six days later, HUVECs in the lower chamber were collected, and RNA was isolated. qRT-PCR confirmed the existence of EBERs in HUVECs, with an EBER1:EBER2 ratio almost identical to that in C666-1 cells (Fig. 2A). To characterize the EVs derived from C666-1 into HUVECs, we first isolated EVs from C666-1 culture supernatant and confirmed their existence and purity by TEM, Zetasizer and Western blotting (Supplemental Fig. 2). After incubation with membrane fluorescent dye PKH67-labeled EVs derived from C666-1 cells, we visualized EVs internalized into endosome-like structures by HUVECs (Fig. 2B). Afterwards, EVs isolated from C666-1 culture supernatant were co-cultured with HUVECs and EBERs were shown being present in both the cytoplasm and nucleus of HUVECs as assayed by ISH with EBER probe (Fig. 2C). Collectively, these observations confirm that EBERs are transferred to surrounding endothelial cells via EVs released by EBV-infected NPC cells.

3.3. EBERs from EVs derived by NPC cells promote angiogenesis

Next, we conducted experiments to investigate the effect of EBERs on endothelial cells. First, Transwell assays indicated that C666-1 in the upper chamber greatly increased the tube-formation capacity of HUVECs in the lower chamber (Fig. 3A, D). The HUVECs co-cultured with EVs isolated from C666-1 culture supernatant were further subjected to tube-formation assay. The result demonstrated that C666-1-derived exosomes could significantly enhance tube formation of HUVECs compared with the control (Fig. 3B, E). q-PCR assay of recovered HUVECs after co-culture with C666-1 cells derived exosomes confirmed transmission of EBERs to HUVECs (Supplementary Fig. 3A). To examine whether EBERs could increase angiogenic ability, we transiently transfected HUVECs with EBER expression plasmids. q-PCR assay of recovered HUVECs confirmed EBERs expression after transfection (Supplementary Fig. 3B). Expression of EBERs in HUVECs could significantly increase their tube-formation, invasion and migration capacity (Fig. 3C, F–H), whereas EBERs did not affect on HUVECs proliferation (Fig. 3I). To confirm this observation, we examined the effect of the EVs from C666-1 with EBERs expression being knockdown. EBER1 expression in C666-1 cells was efficiently reduced with the antisense oligonucleotides (ASOs) complementary to nucleotides 135 to

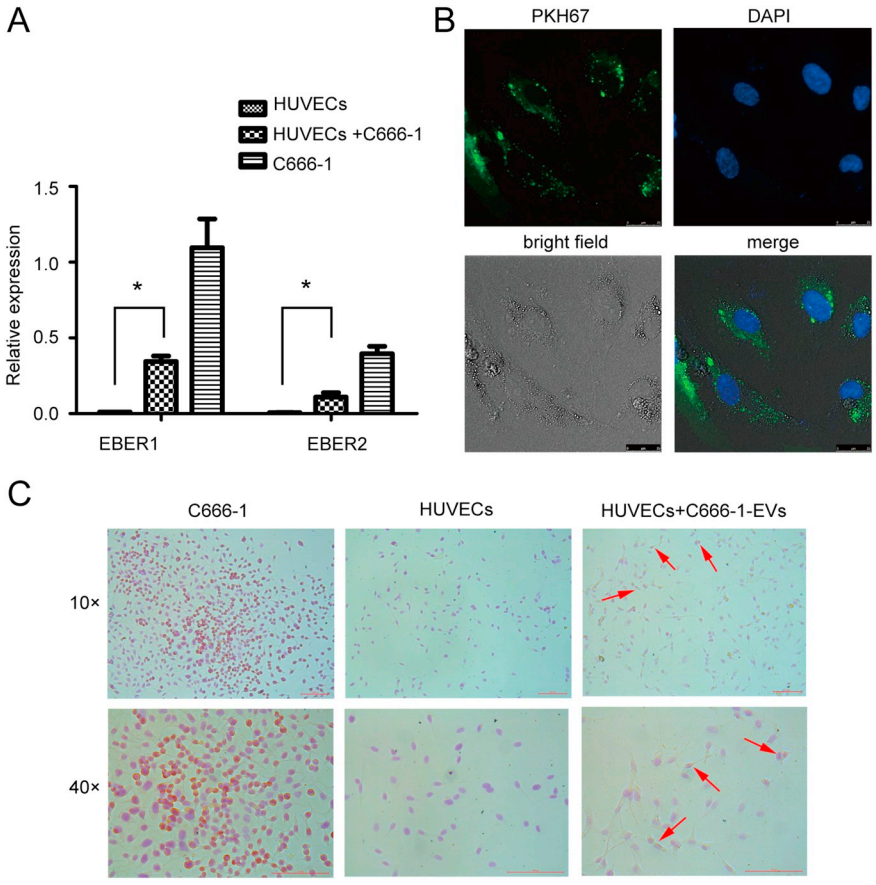

Fig. 2. EBERs are transferred to surrounding endothelial cells via EVs released by EBV-positive NPC cells. (A) EBER levels in HUVECs, untreated or co-cultured for 6 days with C666-1 cells at a 1:4 ratio, separated by Transwell membranes. EBER levels in C666-1 here acted as the positive control. (B) C666-1 EVs were labeled with PKH67 and incubated with HUVECs for 24 h. EV signals were detected in the cytoplasm of HUVECs (green). Nuclear counterstaining was performed using 4′6-diamidino-2-phenylindole (DAPI) (blue). The scale bar indicates 25 μm. (C) Top panel: ISH staining for EBERs was conducted in C666-1 (left) and HUVECs cultured alone (center). C666-1 EVs were incubated with HUVECs for 3 days, after which ISH staining was conducted for EBERs (right). In the enlarged images in the bottom panel, arrows point to EBER-positive cells. The scale bar indicates 100 μm. (A) *P < 0.05, Mann–Whitney test. All experiments were repeated twice.

154 of EBER1, which encompassing stem-loop V of EBER1 (Fig. 3J and Supplementary Fig. 3C). As shown in Fig. 3K, the activity of endothelial cell activation of the EVs isolated from C666-1 with EBER1 knockdown was significantly decreased, evidenced by a decline of VCAM-1 and selectin-E expression, in comparison with the EVs isolated from control ASO treated cells.

To analyze the angiogenic response to EBERs *in vivo*, we performed a Matrigel plug angiogenesis assay to detect the newly formed blood vessels in the transplanted gel plugs in nude mice. The appearance of EBER-transfected cell plugs turned out to be richer in blood vessels than those of the controls (Fig. 4A). The density of neovessels in Matrigel plugs was quantified by immunohistochemical staining (IHC) with anti-human CD31 (Fig. 4B). Quantification analysis confirmed that EBER expression significantly increased angiogenetic vessel formation (Fig. 4C). Thus, EBERs derived from NPC EVs could promote angiogenesis *in vitro* and *in vivo*.

3.4. EBERs derived from NPC exosomes promote angiogenesis by stimulating VCAM-1 expression

To explore molecular events involved in EBER-triggered angiogenesis, we performed RT^2 Profiler PCR array analysis of HUVECs transcripts from the EBERs-transfected cells and the control group. After 48 h post transfection of EBERs expression plasmid, differential expressing angiogenesis-related genes in HUVECs were profiled into 5 groups (Fig. 5A). The volcano plot of the total rank product analysis showed 6 out of 101 genes investigated were significantly upregulated (fold change >2, $P < 0.05$) (Fig. 5B), among which the expression level of VCAM-1 was the highest; western blot analysis further confirmed these observations (Fig. 6A). Considering the markedly altered gene expression level, we selected VCAM1 for further investigation of its involvement in EBERs-triggered angiogenic response. VCAM-1 was first reported to be responsible for the interaction between neutrophils and endothelial cells in the process of inflammation, and subsequently, soluble VCAM-1 was found to contribute to the angiogenic process [31]. To examine the requirement of VCAM-1 in EBER-induced angiogenesis, we first validated the knockdown efficiency of 3 separate siRNAs targeting VCAM-1 and chosen one of the most effective molecules, siVCAM3, for the following experiments (Supplementary Fig. 4A). HUVECs pretreated with the siRNA targeting VCAM-1 for 48 h before challenging them with EBERs plasmid were shown to have an alleviated level of VCAM-1 expression (Fig. 6B) and tube-formation capability (Fig. 6C), whereas the knockdown of VCAM-1 had no observed impact on EBER transfection efficiency (Supplementary Fig. 4B). To further confirm our observation, we established an EBER-expressing cell line by transfecting EBV-negative NPC cells (HNE2). The EVs from the supernatants of both HNE2 and HNE2-EBERs that were pretreated with the siRNA targeting VCAM-1 were shown to lose its ability to promote the tube-formation ability (Fig. 6D). Consistently, the EVs from the EBER1 depleted C666-1 alleviated VCAM-1 expression in HUVECs compared with EVs extracted from untreated C666-1 culture supernatant (Fig. 3K). VCAM-1 is thus at least partially responsible for the angiogenic response stimulated by NPC EV-derived EBERs.

3.5. TLR3 and RIG-I mediate angiogenic capacity conferred by NPC EV-derived EBERs

We have previously reported that the recognition of EBERs by TLR3- and RIG-I could initiate cancer-related inflammation in NPC [13,14] and here our observation indicated exosome-transferred EBERs are

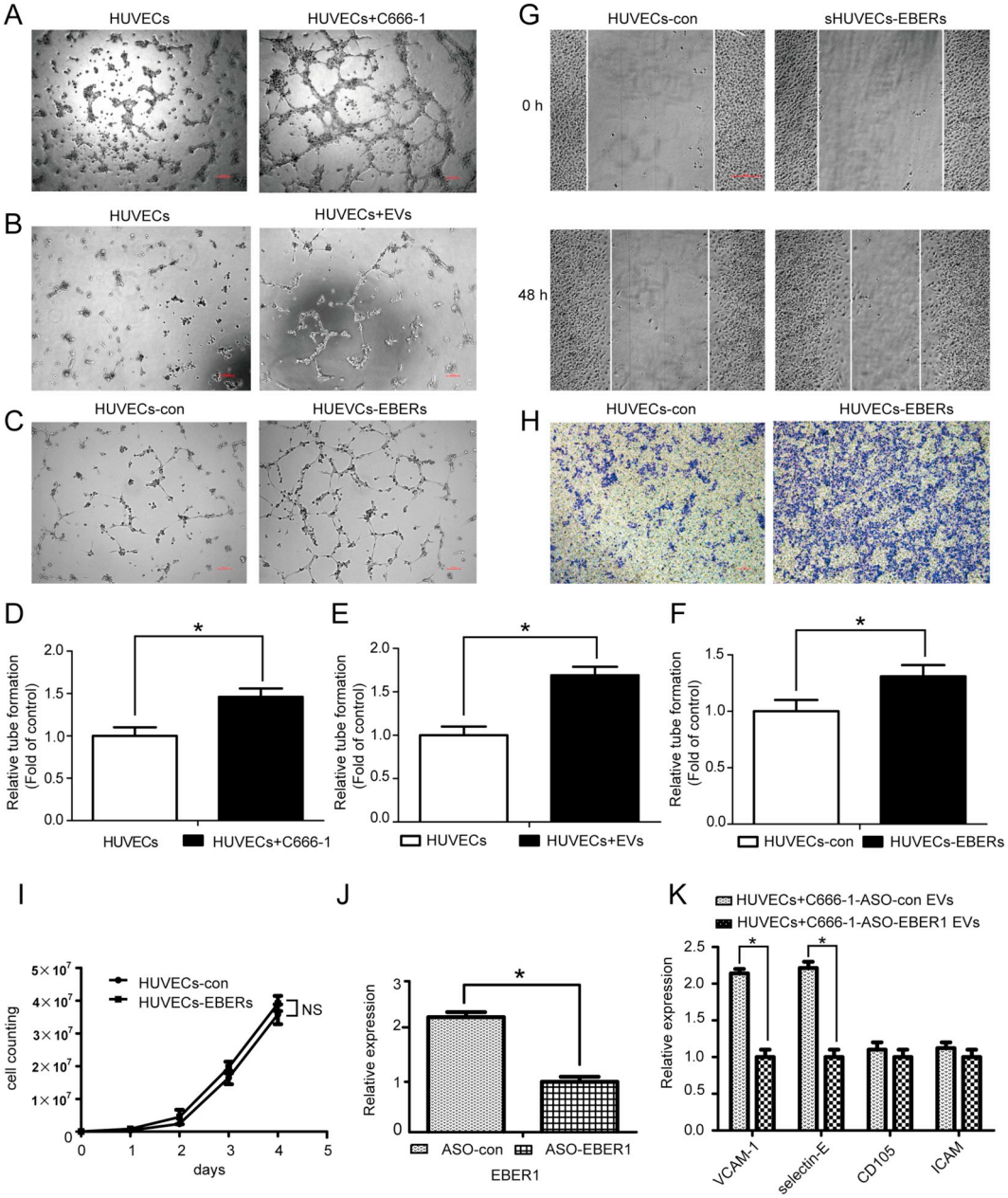

Fig. 3. Exosomal EBERs shed from NPC cells promote angiogenesis. (A) HUVECs were grown alone or in co-culture with C666-1 separated by a 0.4-μm Transwell membrane for 24 h, after which HUVEC tube formation was assayed. The scale bar indicates 100 μm. (B) HUVECs were grown alone or in co-culture with exosomes isolated from C666-1 cells for 24 h, after which HUVEC tube formation was assayed. The scale bar indicates 100 μm. (C) HUVECs were transfected with control or EBER expression plasmids for 24 h, after which HUVEC tube formation was assayed. The scale bar indicates 100 μm. (D–F) Quantification of the number of branch points formed during tubulogenesis determined by pixel density in assays performed in A–C, respectively. (G) Micrographs of the scratch wound healing assay of HUVECs 24 h after transfection with control or EBERs expression plasmid. The scale bar indicates 200 μm. (H) The migratory capability was examined by the Transwell assay using HUVECs 24 h after transfection with control or EBER expression plasmids. Representative images showing cell migration are provided. The scale bar indicates 100 μm. (I) Cell counting was performed for 3 consecutive days for HUVECs transfected with control or EBERs expression plasmid. (J) C666-1 cells were transfected with control ASO or ASO targeting EBER1. 48 h later, RNA was extracted and subjected to qRT-PCR to analyze EBER expression. (K) EVs were isolated from culture supernatant of C666-1 cells which had been transfected with control ASO or ASO targeting EBER1 for 48 h. Then these EVs were co-cultured with HUVECs for 24 h, after which RNA from HUVECs were extracted and subjected to qRT-PCR to analyze the expression of endothelial activation markers. (D–F, I–K) *$P < 0.05$, Mann–Whitney test. All experiments were repeated twice.

located in both the nucleus and cytoplasm (Fig. 2C). Thus, it is reasonable to speculate that the EBERs present in cytoplasm might promote angiogenesis via TLR3 and RIG-I in HUVECs. To test this assumption, we first transfected HUVECs with TLR3/RIG-I shRNA plasmids and validated their interference efficiency in HUVECs (Fig. 7A). Interestingly, TLR3/RIG-I interference substantially alleviated the ability of tube-formation of HUVECs in response to EBERs challenge (Fig. 7B) and we showed that interference had no evident effect on the transfection efficiency of EBERs (Supplementary Fig. 5). Accordingly, after EBERs treatment, VCAM-1 expression was lower in

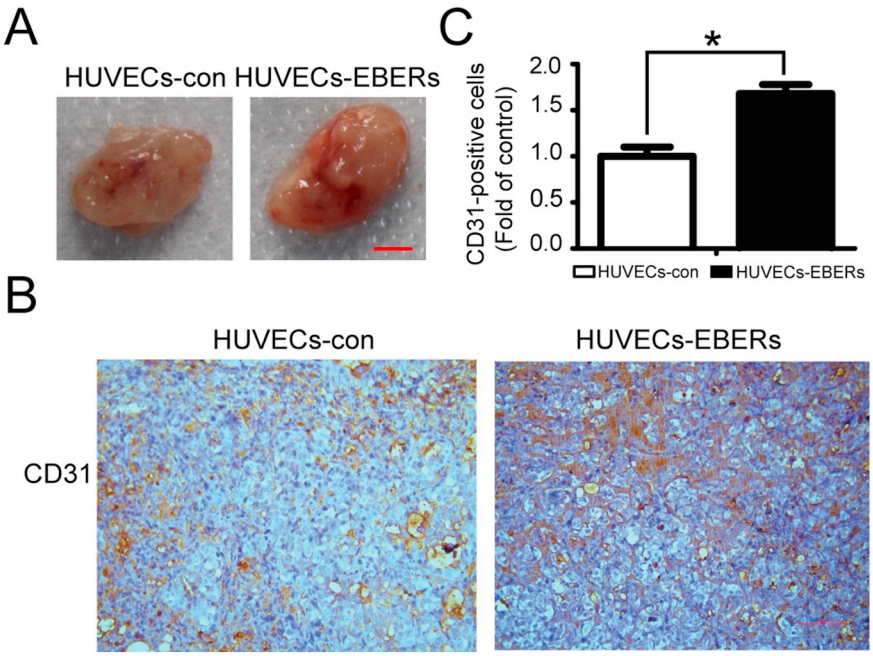

Fig. 4. EBERs promote neovascularization *in vivo*. (A) Representative light microscopic photographs of Matrigel plugs harvested 1 week after subcutaneous injection into nude mice. HUVECs transfected with control or EBERs expression plasmid were mixed with growth factor-reduced Matrigel. The scale bar indicates 2.5 mm. (B) The neovasculature induced by EBERs in Matrigel was visualized by IHC staining of paraffin-embedded tissue sections with anti-human CD31 antibodies. Representative photographs revealed vasculature positively stained for CD31 (brown). The scale bar indicates 100 μm. (C) Quantitative data for the neovessels in Matrigel plugs determined by pixel density between HUVECs transfected with control or EBER expression plasmids (*$P < 0.05$, Mann–Whitney test). Experiments were repeated twice.

TLR3/RIG-I knockdown cells than that in control shRNA plasmid transfected cells (Fig. 7C).

Next, we compared the angiogenic ability of TLR3/RIG-I knockdown HUVECs with the control cells upon treatment with the HNE2-EBER cell-derived exosomes. As expected, TLR3/RIG-I knockdown significantly eliminated VCAM-1 expression of HUVECs after co-culture with EVs from HNE2-EBERs (Fig. 7D). Moreover, ERK (Fig. 7E) rather than NFκB subunit p65 (data not shown) was involved in this process. These findings indicate that TLR3 and RIG-I recognition of EBERs partly accounts for the pro-angiogenic effect of NPC-derived EVs.

Both TLR3 and RIG-I activate downstream signaling pathway via mitogen-activated protein kinase (MAPK), transcription factors nuclear factor-κB (NF-κB) and interferon-regulatory factor 3 (IRF3) [32]. Moreover, VCAM-1 transcription and expression were shown to be increased by NF-κB [32,33] or MAPK pathways [34,35]. Given our data indicated ERK rather than NFκB may be activated in HUVECs by EBERs including EVs secreted by NPC cells (Fig. 8), we investigated whether TLR3 and RIG-I regulate VCAM1 expression via MEK1-ERK1/2 signaling pathway. As shown in Fig. 8A, pretreatment with U0126, a MEK1/2 inhibitor, significantly decreased VCAM-1 expression of HUVECs upon EBERs including EVs treatment. In agreement, ERK-2 knockdown dramatically down-regulated VCAM-1 expression after HUVECs co-cultured with EBERs including EVs (Fig. 8B). Furthermore, ERK-2 knockdown alleviated VCAM-1 transcription activity upon co-culture with EBERs including EVs, as indicated by luciferase reporter gene assay (Fig. 8C), which was validated by q-PCR results (Fig. 8D).

4. Discussion

Recently, EVs and exosomes have been the focus of intensive research owing to their capacity to transfer proteins, miRNAs, and lncRNAs to recipient cells and their crucial roles in signal transduction pathways [22]. A large body of evidence suggests that miRNAs and lncRNAs of human origin can be exchanged between cancer cells and mesenchymal cells [24,25,27] or from cancer stem-like cells and more aggressive cancer cells to the rest of the cancer cells [26,29,30]. Intriguingly, in the present study we provide solid evidence (*in vitro*, *in vivo* and patient samples) showing that EBERs are transferred from EBV-infected NPC cells to surrounding endothelial cells, which stimulates VCAM-1 expression via TLR3/RIG-I recognition (Fig. 9).

VCAM-1 is an immunoglobulin-like molecule that plays a role in various cell-to-cell adhesion interactions, most likely by binding to integrin α4β1 (also known as very late activation antigen-4). VCAM-1 expression is maintained at low levels in endothelial cells of healthy tissues and is stimulated under inflammatory conditions by a multitude of signals such as cytokines, reactive oxygen species, oxidized low-density lipoprotein, TLR agonists, or shear stress [36]. Owing to its involvement in inflammation and its wide distribution in human tissues and organs, VCAM-1 is indicated in autoimmune disease, cardiovascular disease, infections, and cancer [37]. Here, we show that NPC EV-derived EBERs promote angiogenesis by facilitating VCAM-1 expression. In support of this observation, previous publications have shown soluble VCAM-1 to be angiogenic in rat corneas and to confer chemotactic activity to endothelial cells [31]. Furthermore, VCAM-1 was found to mediate angiogenesis upon stimulation by IL-4 and IL-13 [38]. Mechanistically, p38 and FAK, rather than ERK1/2, have been found to account for VCAM-1-stimulated angiogenesis [39], whereas PLC-PKC-NFκB was attributable to VCAM-1 transcription activation [40]. In contrast, we found that EBERs stimulated ERK1/2 rather than NFκB subunit p65 phosphorylation. Furthermore, our results indicated that EBERs stimulate VCAM-1 expression via TLR3 or RIG-I, both of which could transmit downstream signaling pathways mediated by MAPK or NFκB [41]. Of note, a recent report by Fearnley et al. [42] suggests a role for the canonical MAPK pathway involving ERK1/2 and hyperphosphorylation of ATF2 causing elevation in VCAM-1 gene transcription. Our current findings and this relevant published literature lead us to believe that NPC EVs promote angiogenesis via TLR3/RIG-I recognition of EBERs, which is mediated by ERK activated ATF2 rather than NFκB. Interestingly, VEGF-A stimulation of VCAM-1 expression in endothelial cells such as HUVECs has been previously reported by different groups involving multiple mechanisms [33,42–44]. Accordingly, in addition to EBERs, protein-based factors associated with EVs from NPC cells, such as VEGF-A may promote such signaling leading to increased VCAM-1 gene transcription, which exemplified the significance of VCAM-1 in NPC EVs mediated angiogenesis.

Besides its association with tumor angiogenesis, EBER-mediated

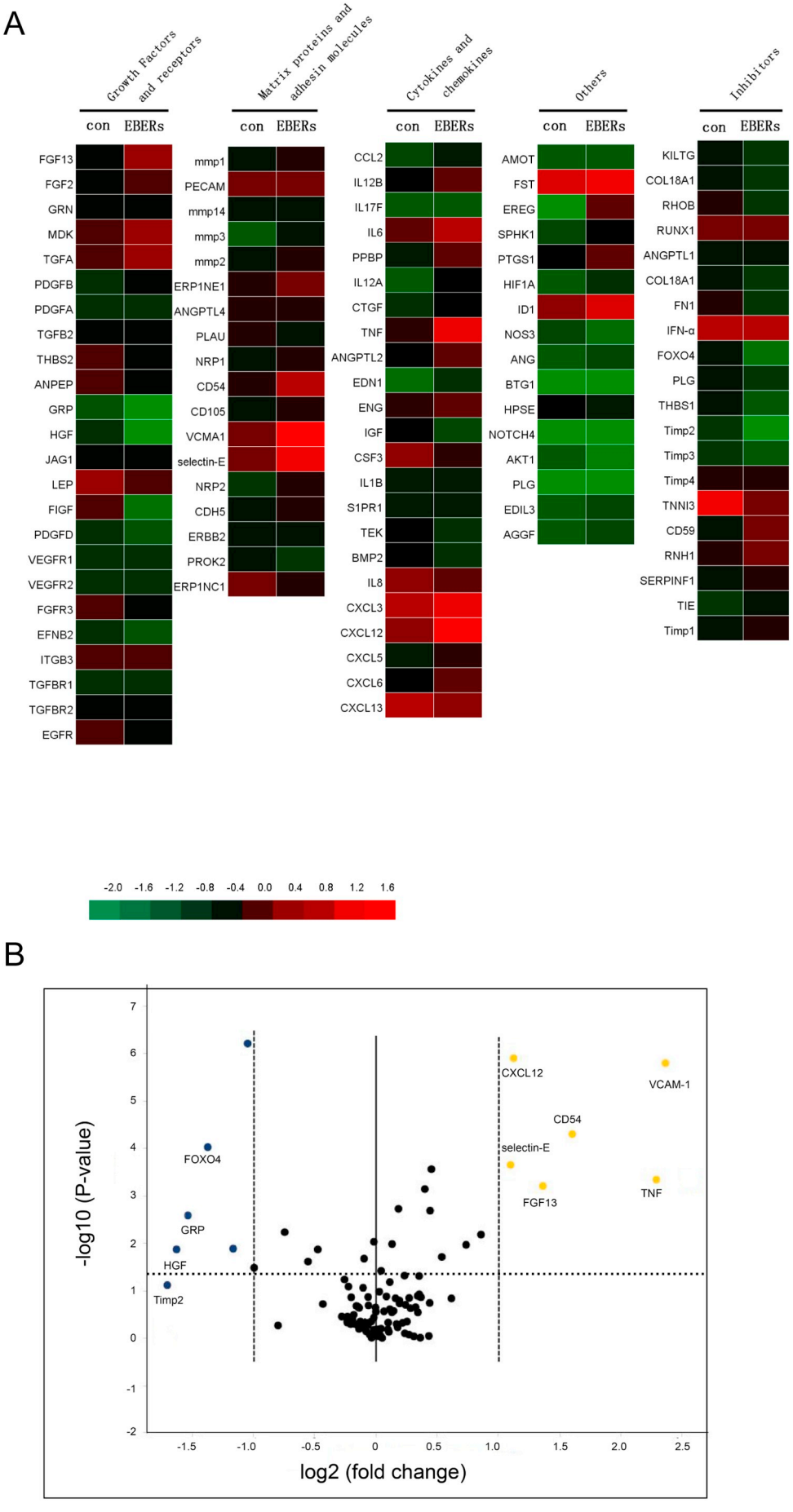

Fig. 5. PCR array of angiogenesis related genes indicates VCAM-1 expression is significantly increased after challenging HUVECs with EBERs. (A) EBERs shed from EVs of NPC cells promote angiogenesis. Heatmap illustrating changes in mRNA expression levels (log2 transformed) between HUVECs transfected with control or EBERs expression plasmids. Differentially expressed genes fell into 5 groups according to their molecular characteristics or their association with angiogenesis. Each value is an average of 3 independent experiments, with values presented from low (green) to high (red). (B) Volcano plot of mRNA changes across HUVECs transfected with control or EBERs expression plasmids. All experiments were repeated twice.

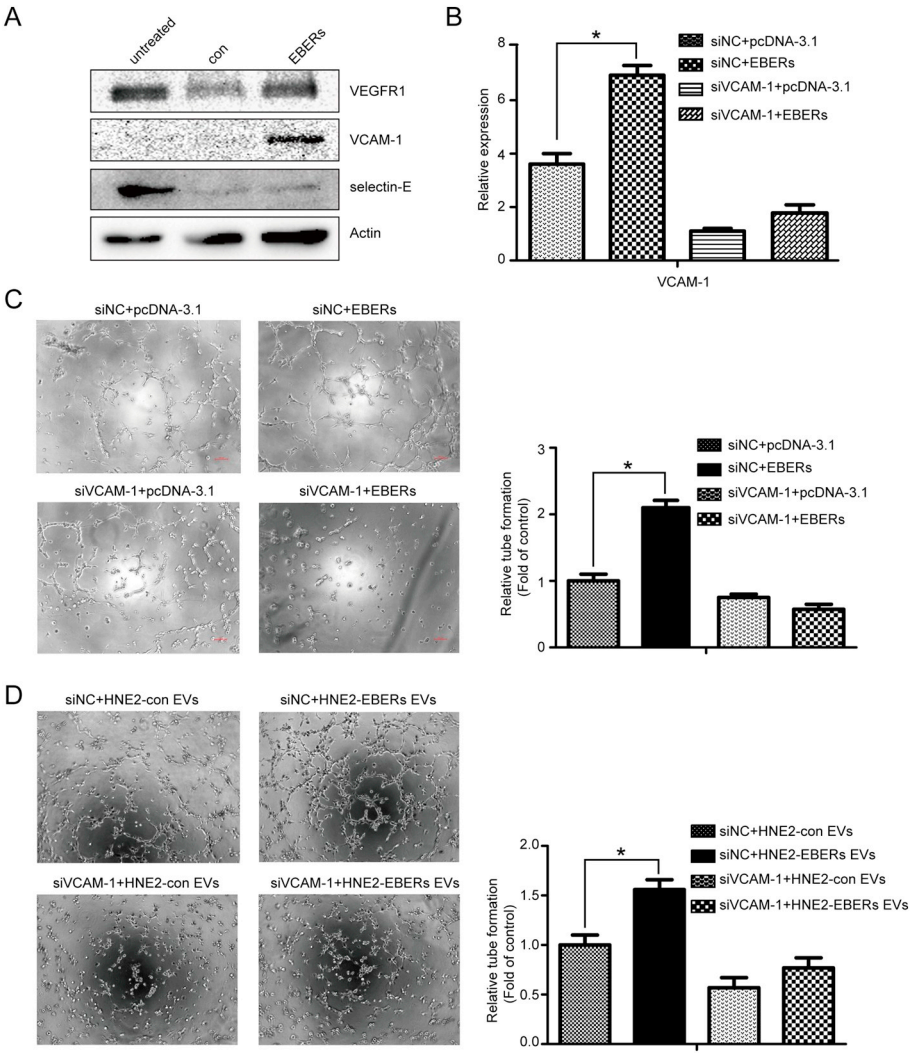

Fig. 6. EBERs derived from NPC exosomes promote angiogenesis by stimulating VCAM-1 expression. (A) HUVECs were transfected with control or EBERs expression plasmids. After 24 h, proteins were extracted and subjected to WB analysis of angiogenic markers in these 2 groups. (B–C) HUVECs were transfected with control or siRNA targeting VCAM-1 for 48 h, after which control or EBERs expression plasmids were applied to challenge HUVECs for another 24 h. RNA was extracted, and VCAM-1 expression was analyzed by qRT-PCR (B), and tube formation assay was performed (C, left) between these 2 groups. The number of branch points formed during tubulogenesis was determined by pixel density (C, right). (D) HUVECs were transfected with control RNA or siRNA targeting VCAM-1 for 48 h, after which EVs isolated from culture supernatant of HNE2-control or HNE2-EBER expression cell lines were applied to the co-culture for another 24 h. The tube formation assay was then performed in these 2 groups. The formation of tubelike structures was observed with phase contrast microscopy (left) and quantified by pixel density (right). (B-D) *P < 0.05, Mann–Whitney test. (C–D) The scale bar indicates 100 μm. All experiments were repeated twice.

VCAM-1 expression might contribute to tumor progression in various ways. The last few years have witnessed an ever-increasing body of knowledge on the molecular understanding of tumorigenicity and metastasis, and an impressive variety of VCAM-1 functionalities in cancer have been elucidated. Endothelial VCAM-1 has been found to mediate tumor cell adhesion, transendothelial migration, and myeloid cell adhesion, all of which collectively predispose tissues to tumor metastasis [36]. EBV is closely related to NPC metastasis, however, previous research has concentrated on understanding this association by focusing on mechanisms of EBV-encoded proteins and RNAs within tumor cells. Furthermore, although recent *in vitro* evidence suggests that NPC cells can communicate with endothelial cells via exosomes [23], the impact of exosome-derived EBERs on endothelial cells located in NPC parenchymal tissues and the underlying molecular mechanisms are not fully understood. Our present research demonstrated the association between EBERs and VCAM-1 via TLR3/RIG-I-mediated transcription activation, illustrating the impact of NPC EV-derived EBERs on tumor angiogenesis. EBER-stimulated VCAM-1 per se was verified to be angiogenic in the present study, and the stimulation of VCAM-1 might further directly contribute to metastasis by promoting tumor cell adhesion, transendothelial migration, and myeloid cell recruitment and adhesion, which affect primary tumor metastasis [45,46]. Hence, the causal relationship between EBERs and VCAM-1 may be vital for NPC metastasis, which should be the focus of further study.

EBV is a γ-herpesvirus that has been a leading candidate implicated in triggering several autoimmune diseases and cancer. Apart from its capability to infect epithelial cells and lymphocytes, it can infect endothelial cells or fibroblasts *in vitro* [31,47,48]. This seems to contradict our results by raising the possibility of EBV infection rather than EVs accounting for the presence of EBERs in endothelial cells in NPC parenchymal tissues. We propose the following explanations in support of our results. First, IHC staining indicated that EBV-encoded LMP1 never appeared in the epithelial cells of NPC tissues, in contrast to the detection of LMP1 in EBV-infected fibroblasts in systemic sclerosis [48]. Second, most of the published reports investigated the infection of endothelial cells by EBV with *in vitro* models and did not validate their hypothesis with clinical samples [47,49]. Third, EBERs positive endothelial cells were only evident in the vicinity of some EBERs intensively stained NPC cells, while there were no presence of EBERs in most endothelial cells in EBV positive NPC parenchymal tissues. Finally, despite the possibilities of EBV infection, EVs derived from EBV positive NPC cells are capable of delivering exosomes to co-cultured endothelial cells [23,50], which is reminiscent of our observation that EVs-derived EBERs were proven to be angiogenic.

To our knowledge, this is the first report on viral noncoding RNAs being transferred from cancer cells to endothelial cells via EVs, thereby

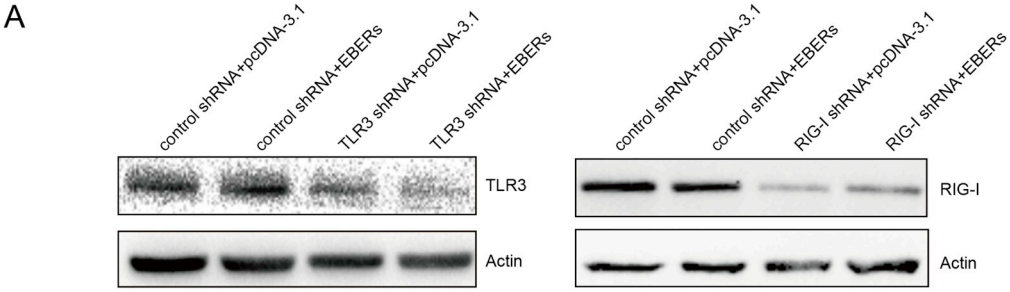

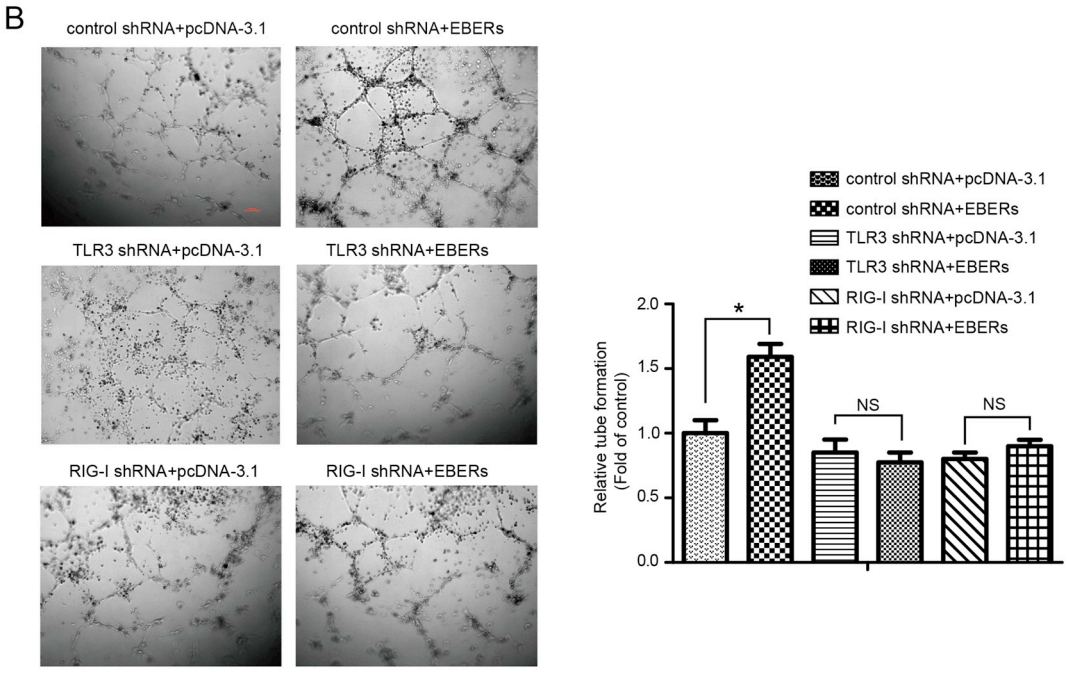

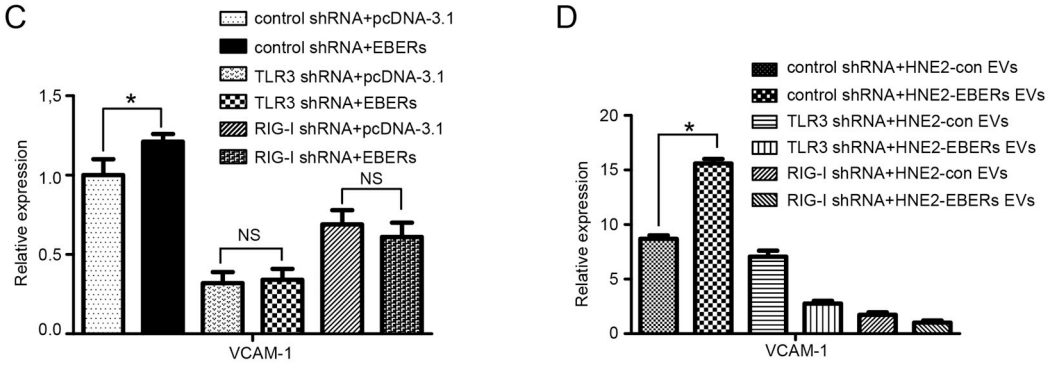

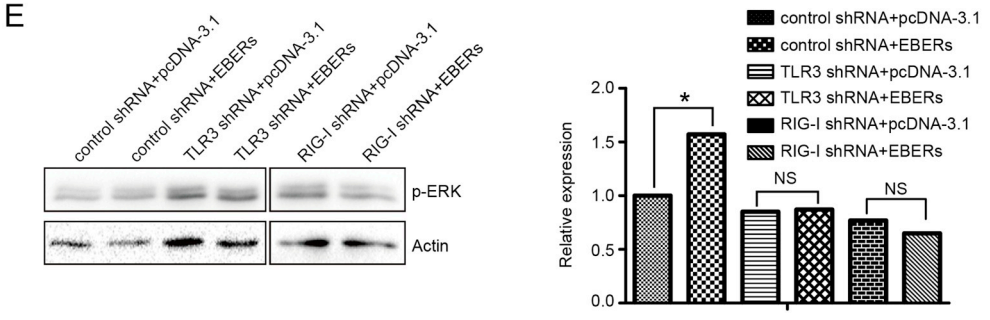

(caption on next page)

Fig. 7. TLR3 and RIG-I mediate angiogenic capacity conferred by NPC EV-derived EBERs. (A–C) HUVECs were transfected with TLR3/RIG-I shRNA plasmids for 48 h, after which control or EBER expression plasmids were used to challenge HUVECs for another 24 h. (A) Proteins were extracted, and TLR3/RIG-I knockdown efficiency was validated by western blotting analysis. (B) The formation of tubelike structures was observed with phase contrast microscopy (left) and quantified by pixel density (right). The scale bar indicates 100 μm. (C) Next, RNA was extracted, and VCAM-1 expression was analyzed by qRT-PCR. (D) HUVECs were transfected with TLR3/RIG-I shRNA plasmids for 48 h, after which EVs isolated from the culture supernatant of HNE2-control or HNE2-EBER cells were applied to the co-culture for another 24 h. RNA was extracted, and VCAM-1 expression was analyzed by qRT-PCR. (E) HUVECs were transfected with TLR3/RIG-I shRNA plasmids for 48 h, after which control or EBERs expression plasmids were used to challenge HUVECs for another 24 h. Proteins were extracted, phosphorylated ERK was analyzed by western blot assay (left) and subjected to densitometric analysis (right). (B-E) *P < 0.05, Mann–Whitney test. All experiments were repeated twice.

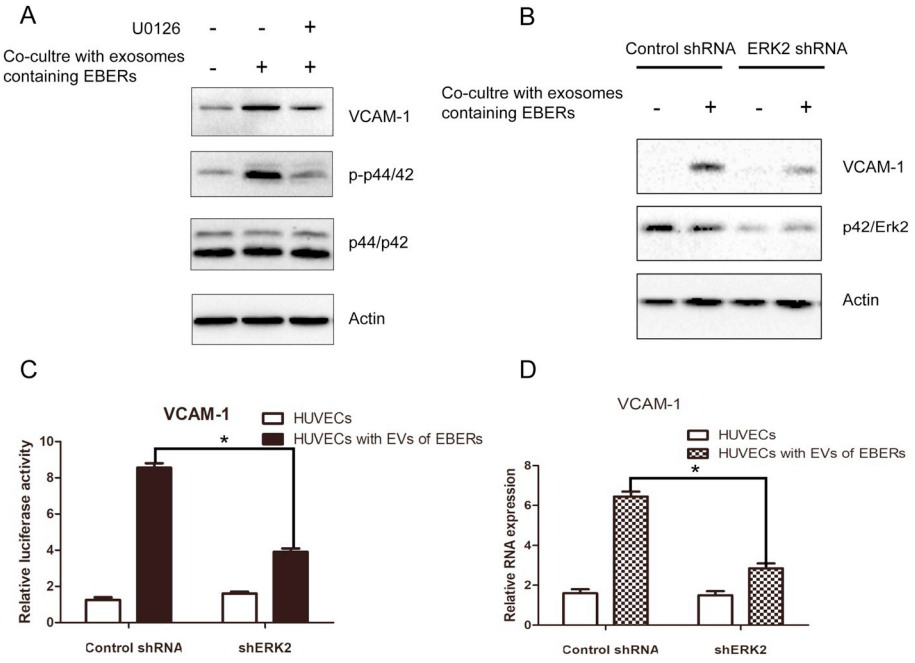

Fig. 8. MEK1-ERK1/2 pathway is required for EBERs containing EVs induced VCAM1 expression. (A) EVs were isolated from the culture supernatant of HNE2-EBERs. HUVECs were cultured alone or co-cultured with EVs in the presence or absence of U0126, a MEK1/2 inhibitor for 48 h, after which protein of HUVECs were isolated and subjected to Western blot to analyze VCAM-1 activation. (B) HUVECs knock-down ERK2 expression or expressing a scramble shRNA sequence were cultured alone or co-cultured with EVs isolated from the culture supernatant of HNE2-EBERs for 48 h. Then protein of HUVECs were isolated and subjected to Western blot to analyze VCAM-1 activation. (C) HUVECs transfected with VCAM-1 promoter guided luciferase reporter gene plasmid were cultured alone or co-cultured with EVs isolated from the culture supernatant of HNE2-EBERs for 48 h, after which HUVECs were lysed and subjected to reporter gene assays. (D) Control shRNA or ERK2 shRNA expressing HUVECs were cultured alone or co-cultured with EVs isolated from the culture supernatant of HNE2-EBERs for 48 h. Then RNAs of HUVECs were isolated and subjected to q-PCR to analyze VCAM-1 transcription. (C–D) *P < 0.05, Mann–Whitney test. All experiments were repeated twice.

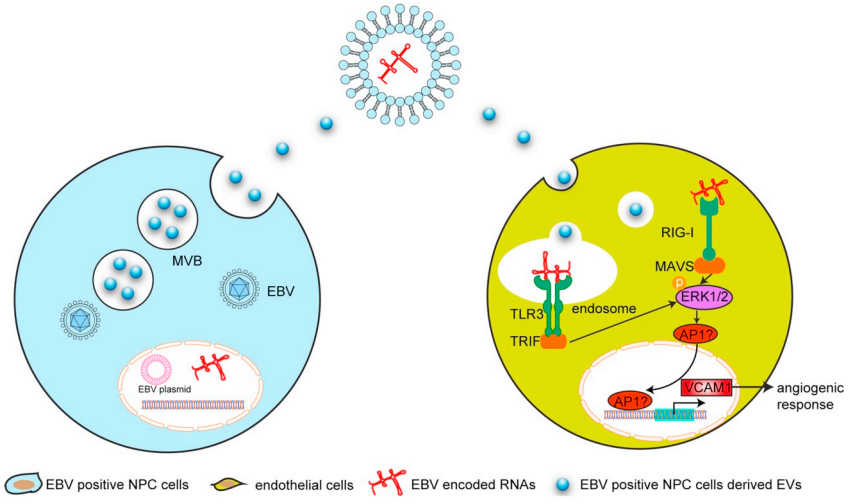

Fig. 9. A schematic diagram showing EVs derived EBERs promote angiogenesis via TLR3/RIG-I-mediated VCAM-1 expression.

promoting subsequent angiogenesis. This scenario might be also applicable for other EBV-mediated tumor-promoting angiogenesis phenomena such as gastric carcinoma. We expect that this newly revealed role of EV-derived EBERs in modulating NPC angiogenesis could eventually help identify potential targets in EBV associated epithelial carcinoma treatment from the perspective of tumor and microenvironment interplay. Further studies need to investigate the relationship between EBERs and VCAM-1 in NPC metastasis.

Supplementary data to this article can be found online at https://doi.org/10.1016/j.bbadis.2019.01.015.

Transparency document

The Transparency document associated with this article can be found in online version.

Acknowledgments

This work was supported by grants from the National Key Basic Research Program of the Chinese Ministry of Science and Technology (2013CB967203), the Natural Science Foundation of China, (91129709, 81602405, 81874200, 81572750 and 81602406), Hunan Department of Science and Technology Foundation of China (2015JC3026), Innovation-driven Program of the Central South University (20170033010007) and Key Projects in the National Science & Technology Pillar Program (2013BAI01B07).

Disclosure of potential conflicts of interest

The authors declare no conflict of interest.

References

[1] M.R. Lerner, N.C. Andrews, G. Miller, J.A. Steitz, Two small RNAs encoded by Epstein-Barr virus and complexed with protein are precipitated by antibodies from patients with systemic lupus erythematosus, Proc. Natl. Acad. Sci. U. S. A. 78 (1981) 805–809.
[2] M.D. Rosa, E. Gottlieb, M.R. Lerner, J.A. Steitz, Striking similarities are exhibited by two small Epstein-Barr virus-encoded ribonucleic acids and the adenovirus-associated ribonucleic acids VAI and VAII, Mol. Cell. Biol. 1 (1981) 785–796.
[3] D. Iwakiri, L. Zhou, M. Samanta, M. Matsumoto, T. Ebihara, T. Seya, S. Imai, M. Fujieda, K. Kawa, K. Takada, Epstein-Barr virus (EBV)-encoded small RNA is released from EBV-infected cells and activates signaling from toll-like receptor 3, J. Exp. Med. 206 (2009) 2091–2099.
[4] M. Samanta, D. Iwakiri, T. Kanda, T. Imaizumi, K. Takada, EB virus-encoded RNAs are recognized by RIG-I and activate signaling to induce type I IFN, EMBO J. 25 (2006) 4207–4214.
[5] A. Nanbo, K. Inoue, K. Adachi-Takasawa, K. Takada, Epstein–Barr virus RNA confers resistance to interferon-α-induced apoptosis in Burkitt's lymphoma, EMBO J. 21 (2002) 954–965.
[6] A. Nanbo, H. Yoshiyama, K. Takada, Epstein-Barr virus-encoded poly (A)− RNA confers resistance to apoptosis mediated through Fas by blocking the PKR pathway in human epithelial intestine 407 cells, J. Virol. 79 (2005) 12280–12285.
[7] D.P. Toczyski, A.G. Matera, D.C. Ward, J.A. Steitz, The Epstein-Barr virus (EBV) small RNA EBER1 binds and relocalizes ribosomal protein L22 in EBV-infected human B lymphocytes, Proc. Natl. Acad. Sci. U. S. A. 91 (1994) 3463–3467.
[8] G. Gregorovic, R. Bosshard, C.E. Karstegl, R.E. White, S. Pattle, A.K. Chiang, O. Dittrich-Breiholz, M. Kracht, R. Russ, P.J. Farrell, Cellular gene expression that correlates with EBER expression in Epstein-Barr virus-infected lymphoblastoid cell lines, J. Virol. 85 (2011) 3535–3545.
[9] N. Lee, G. Pimienta, J.A. Steitz, AUF1/hnRNP D is a novel protein partner of the EBER1 noncoding RNA of Epstein-Barr virus, RNA 18 (2012) 2073–2082.
[10] A.R. Pont, N. Sadri, S.J. Hsiao, S. Smith, R.J. Schneider, mRNA decay factor AUF1 maintains normal aging, telomere maintenance, and suppression of senescence by activation of telomerase transcription, Mol. Cell 47 (2012) 5–15.
[11] N. Lee, W.N. Moss, T.A. Yario, J.A. Steitz, EBV noncoding RNA binds nascent RNA to drive host PAX5 to viral DNA, Cell 160 (2015) 607–618.
[12] K.T. Tycowski, Y.E. Guo, N. Lee, W.N. Moss, T.K. Vallery, M. Xie, J.A. Steitz, Viral noncoding RNAs: more surprises, Genes Dev. 29 (2015) 567–584.
[13] Z. Li, Y. Duan, S. Cheng, Y. Chen, Y. Hu, L. Zhang, J. He, Q. Liao, L. Yang, L.Q. Sun, EBV-encoded RNA via TLR3 induces inflammation in nasopharyngeal carcinoma, Oncotarget 6 (2015) 24291–24303.
[14] Y. Duan, Z. Li, S. Cheng, Y. Chen, L. Zhang, J. He, Q. Liao, L. Yang, Z. Gong, L.Q. Sun, Nasopharyngeal carcinoma progression is mediated by EBER-triggered inflammation via the RIG-I pathway, Cancer Lett. 361 (2015) 67–74.
[15] S. Swaminathan, B. Tomkinson, E. Kieff, Recombinant Epstein-Barr virus with small RNA (EBER) genes deleted transforms lymphocytes and replicates in vitro, Proc. Natl. Acad. Sci. 88 (1991) 1546–1550.
[16] M. Yajima, T. Kanda, K. Takada, Critical role of Epstein-Barr Virus (EBV)-encoded RNA in efficient EBV-induced B-lymphocyte growth transformation, J. Virol. 79 (2005) 4298–4307.
[17] W. Ahmed, P.S. Philip, S. Tariq, G. Khan, Epstein-Barr virus-encoded small RNAs (EBERs) are present in fractions related to exosomes released by EBV-transformed cells, PLoS One 9 (2014) e99163.
[18] D. Hanahan, R.A. Weinberg, Hallmarks of cancer: the next generation, Cell 144 (2011) 646–674.
[19] S.M. Weis, D.A. Cheresh, Tumor angiogenesis: molecular pathways and therapeutic targets, Nat. Med. 17 (2011) 1359–1370.
[20] J.K. Liao, Linking endothelial dysfunction with endothelial cell activation, J. Clin. Invest. 123 (2013) 540–541.
[21] A.E. Koch, M.M. Halloran, C.J. Haskell, M.R. Shah, P.J. Polverini, Angiogenesis mediated by soluble forms of E-selectin and vascular cell adhesion molecule-1, Nature 376 (1995) 517–519.
[22] M. Tkach, C. Thery, Communication by extracellular vesicles: where we are and where we need to go, Cell 164 (2016) 1226–1232.
[23] D.G. Meckes Jr., K.H. Shair, A.R. Marquitz, C.P. Kung, R.H. Edwards, N. Raab-Traub, Human tumor virus utilizes exosomes for intercellular communication, Proc. Natl. Acad. Sci. U. S. A. 107 (2010) 20370–20375.
[24] G. Zhuang, X. Wu, Z. Jiang, I. Kasman, J. Yao, Y. Guan, J. Oeh, Z. Modrusan, C. Bais, D. Sampath, N. Ferrara, Tumour-secreted miR-9 promotes endothelial cell migration and angiogenesis by activating the JAK-STAT pathway, EMBO J. 31 (2012) 3513–3523.
[25] H. Tadokoro, T. Umezu, K. Ohyashiki, T. Hirano, J.H. Ohyashiki, Exosomes derived from hypoxic leukemia cells enhance tube formation in endothelial cells, J. Biol. Chem. 288 (2013) 34343–34351.
[26] M.T. Le, P. Hamar, C. Guo, E. Basar, R. Perdigao-Henriques, L. Balaj, J. Lieberman, miR-200-containing extracellular vesicles promote breast cancer cell metastasis, J. Clin. Invest. 124 (2014) 5109–5128.
[27] T. Umezu, H. Tadokoro, K. Azuma, S. Yoshizawa, K. Ohyashiki, J.H. Ohyashiki, Exosomal miR-135b shed from hypoxic multiple myeloma cells enhances angiogenesis by targeting factor-inhibiting HIF-1, Blood 124 (2014) 3748–3757.
[28] S.T. Cheung, D.P. Huang, A.B. Hui, K.W. Lo, C.W. Ko, Y.S. Tsang, N. Wong, B.M. Whitney, J.C. Lee, Nasopharyngeal carcinoma cell line (C666-1) consistently harbouring Epstein-Barr virus, Int. J. Cancer 83 (1999) 121–126.
[29] K. Takahashi, I.K. Yan, T. Kogure, H. Haga, T. Patel, Extracellular vesicle-mediated transfer of long non-coding RNA ROR modulates chemosensitivity in human hepatocellular cancer, FEBS Open Bio 4 (2014) 458–467.
[30] A. Conigliaro, V. Costa, A. Lo Dico, L. Saieva, S. Buccheri, F. Dieli, M. Manno, S. Raccosta, C. Mancone, M. Tripodi, G. De Leo, R. Alessandro, CD90+ liver cancer cells modulate endothelial cell phenotype through the release of exosomes containing H19 lncRNA, Mol. Cancer 14 (2015) 155.
[31] A.E. Koch, M.M. Halloran, C.J. Haskell, M.R. Shah, P.J. Polverini, Angiogenesis Mediated by Soluble Forms of E-selectin and Vascular Cell-Adhesion Molecule-1, (1995).
[32] J.S. Arthur, S.C. Ley, Mitogen-activated protein kinases in innate immunity, Nat. Rev. Immunol. 13 (2013) 679–692.
[33] I. Kim, S.O. Moon, S.H. Kim, H.J. Kim, Y.S. Koh, G.Y. Koh, Vascular endothelial growth factor expression of intercellular adhesion molecule 1 (ICAM-1), vascular cell adhesion molecule 1 (VCAM-1), and E-selectin through nuclear factor-kappa B activation in endothelial cells, J. Biol. Chem. 276 (2001) 7614–7620.
[34] C.W. Lee, W.N. Lin, C.C. Lin, S.F. Luo, J.S. Wang, J. Pouyssegur, C.M. Yang, Transcriptional regulation of VCAM-1 expression by tumor necrosis factor-alpha in human tracheal smooth muscle cells: involvement of MAPKs, NF-kappaB, p300, and histone acetylation, J. Cell. Physiol. 207 (2006) 174–186.
[35] S.F. Luo, R.Y. Fang, H.L. Hsieh, P.L. Chi, C.C. Lin, L.D. Hsiao, C.C. Wu, J.S. Wang, C.M. Yang, Involvement of MAPKs and NF-kappaB in tumor necrosis factor alpha-induced vascular cell adhesion molecule 1 expression in human rheumatoid arthritis synovial fibroblasts, Arthritis Rheum. 62 (2010) 105–116.
[36] M. Schlesinger, G. Bendas, Vascular cell adhesion molecule-1 (VCAM-1)—an increasing insight into its role in tumorigenicity and metastasis, Int. J. Cancer 136 (2015) 2504–2514.
[37] A. Salajegheh, Vascular Cell Adhesion Molecule-1 (VCAM-1), Angiogenesis in Health, Disease and Malignancy, Springer, 2016, pp. 375–379 (Place Published).
[38] J.-i. Fukushi, M. Ono, W. Morikawa, Y. Iwamoto, M. Kuwano, The activity of soluble VCAM-1 in angiogenesis stimulated by IL-4 and IL-13, J. Immunol. 165 (2000) 2818–2823.
[39] S. Nakao, T. Kuwano, T. Ishibashi, M. Kuwano, M. Ono, Synergistic effect of TNF-α in soluble VCAM-1-induced angiogenesis through α4 integrins, J. Immunol. 170 (2003) 5704–5711.
[40] I. Kim, S.-O. Moon, S.H. Kim, H.J. Kim, Y.S. Koh, G.Y. Koh, Vascular endothelial growth factor expression of intercellular adhesion molecule 1 (ICAM-1), vascular cell adhesion molecule 1 (VCAM-1), and E-selectin through nuclear factor-κB activation in endothelial cells, J. Biol. Chem. 276 (2001) 7614–7620.
[41] S.W. Brubaker, K.S. Bonham, I. Zanoni, J.C. Kagan, Innate immune pattern recognition: a cell biological perspective, Annu. Rev. Immunol. 33 (2015) 257–290.
[42] G.W. Fearnley, A.F. Odell, A.M. Latham, N.A. Mughal, A.F. Bruns, N.J. Burgoyne, S. Homer-Vanniasinkam, I.C. Zachary, M.C. Hollstein, S.B. Wheatcroft, S. Ponnambalam, VEGF-A isoforms differentially regulate ATF-2-dependent VCAM-1 gene expression and endothelial-leukocyte interactions, Mol. Biol. Cell 25 (2014) 2509–2521.
[43] R.K. Jain, G.C. Koenig, M. Dellian, D. Fukumura, L.L. Munn, R.J. Melder, Leukocyte-endothelial adhesion and angiogenesis in tumors, Cancer Metastasis Rev. 15 (1996) 195–204.
[44] M.R. Abid, S.C. Shih, H.H. Otu, K.C. Spokes, Y. Okada, D.T. Curiel, T. Minami, W.C. Aird, A novel class of vascular endothelial growth factor-responsive genes that require forkhead activity for expression, J. Biol. Chem. 281 (2006) 35544–35553.

[45] A.M. Gil-Bernabe, S. Ferjancic, M. Tlalka, L. Zhao, P.D. Allen, J.H. Im, K. Watson, S.A. Hill, A. Amirkhosravi, J.L. Francis, J.W. Pollard, W. Ruf, R.J. Muschel, Recruitment of monocytes/macrophages by tissue factor-mediated coagulation is essential for metastatic cell survival and premetastatic niche establishment in mice, Blood 119 (2012) 3164–3175.
[46] S. Ferjancic, A.M. Gil-Bernabe, S.A. Hill, P.D. Allen, P. Richardson, T. Sparey, E. Savory, J. McGuffog, R.J. Muschel, VCAM-1 and VAP-1 recruit myeloid cells that promote pulmonary metastasis in mice, Blood 121 (2013) 3289–3297.
[47] C. Casiraghi, K. Dorovini-Zis, M.S. Horwitz, Epstein-Barr virus infection of human brain microvessel endothelial cells: a novel role in multiple sclerosis, J. Neuroimmunol. 230 (2011) 173–177.
[48] A. Farina, M. Cirone, M. York, S. Lenna, C. Padilla, S. McLaughlin, A. Faggioni, R. Lafyatis, M. Trojanowska, G.A. Farina, Epstein-Barr virus infection induces aberrant TLR activation pathway and fibroblast-myofibroblast conversion in scleroderma, J. Invest. Dermatol. 134 (2014) 954–964.
[49] K. Jones, C. Rivera, C. Sgadari, J. Franklin, E.E. Max, K. Bhatia, G. Tosato, Infection of human endothelial cells with Epstein-Barr virus, J. Exp. Med. 182 (1995) 1213–1221.
[50] Y.K. Chan, H. Zhang, P. Liu, S.W. Tsao, M.L. Lung, N.K. Mak, R. Ngok-Shun Wong, P. Ying-Kit Yue, Proteomic analysis of exosomes from nasopharyngeal carcinoma cell identifies intercellular transfer of angiogenic proteins, Int. J. Cancer 137 (2015) 1830–1841.
[51] Z. Li, S. Fu, L.Q. Sun, Viral Noncoding RNAs in Cancer Biology, Adv. Exp. Med. Biol. 927 (2016) 367–389.
[52] X. Lin, S. Liu, X. Luo, X. Ma, L. Guo, L. Li, Z. Li, Y. Tao, Y. Cao, EBV-encoded LMP1 regulates Op18/stathmin signaling pathway by cdc2 mediation in nasopharyngeal carcinoma cells, Int. J. Cancer 124 (2009) 1020–1027.
[53] J. Lu, M. Tang, H. Li, Z. Xu, X. Weng, J. Li, X. Yu, L. Zhao, H. Liu, Y. Hu, Z. Tan, L. Yang, M. Zhong, J. Zhou, J. Fan, A.M. Bode, W. Yi, J. Gao, L. Sun, Y. Cao, EBV-LMP1 suppresses the DNA damage response through DNA-PK/AMPK signaling to promote radioresistance in nasopharyngeal carcinoma, Cancer Lett. 380 (2016) 191–200.